

Unusual reaction paths of S_N2 nucleophile substitution reactions CH₄+H⁻→CH₄+H⁻ and CH₄+F⁻→CH₃F+H⁻: Quantum chemical calculations

Ruslan M. Minyaev ^{a,*}, Wolfgang Quapp ^{b,*}, Benjamin Schmidt ^b,
Ilya V. Getmanskii ^a, Vitaliy V. Koval ^a

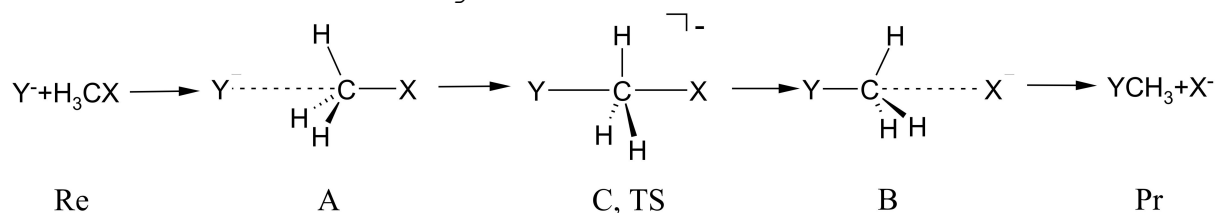
^a *Institute of Physical and Organic Chemistry, Southern Federal University, 194/2 Stachka Ave., Rostov-on-Don 344090, Russian Federation;*

^b *Leipzig University, Mathematical Institute, Augustusplatz, D-04109 Leipzig, Germany*

Quantum chemical (CCSD(full)/6-311++G(3df,2pd), CCSD(T)(full)/6-311++G(3df,2pd)) and density function theory (B3LYP/6-311++G(3df,3pd)) calculations were performed for the S_N2 nucleophile substitution reactions CH₄+H⁻→CH₄+H⁻ and CH₄+F⁻→CH₃F+H⁻. The calculated gradient reaction pathways for both reactions have an unusual behavior. An unusual saddle point of index 2 lies on the gradient reaction path. Using Newton trajectories for the reaction path, we can detect VRI point at which the reaction path branches.

1. Introduction

Mechanisms of a gas-phase bimolecular nucleophilic substitution at the tetrahedral carbon atom [1] are well studied experimentally [2-6] and theoretically [1,7-18]. However their reaction pathways on the corresponding potential energy surface (PES) may be quite complex [15,17] and they remain not studied enough.



The paths of such reactions begin with the formation of the pre-reaction complex (intermediate) **A** of reagents (**Re**) which usually corresponds to a minimum on the potential energy surface (PES) of the system. Then pathways pass through the transition state **C** corresponding to the saddle point on the PES, and terminate at the minimum corresponding to the second pre-reaction (intermediate) complex **B** of products (**Pr**). The energy profile of this reaction has a simple double-well form, separated by an energy barrier. The pathway of a

reaction, according to various calculations, is observed for almost all studied nucleophiles X, Y [1-18]. Although the distribution of stationary points (minima and saddle points) can be quite complicated on the PES in the reaction zone [15,17].

It was shown earlier [19] that the chemical system can infinitesimally slowly slide down on the PES along gradient lines (steepest descent lines), which, like equipotential lines, cannot branch outside of stationary points. Such a path goes downhill in both directions of the transition vector at the saddle point on the PES and enters the adjacent stationary points. It is called gradient reaction path [19]. The gradient reaction pathway is similar to the IRC [20] in the case of Cartesian coordinates with mass weighting. It is well adapted to the topology of the PES, which is observed for almost all the studied gas phase S_N2 reactions [1-18]. However, when the PES topology has a more complex structure, gradient lines are not fine enough [21-25].

In this paper we discuss a case where nucleophiles X, Y are the hydride anions X, Y = H, or hydride and fluoride anions X = H-, Y = F-. The IRC path which is supposed as a smooth continuous line, connects the saddle point of index one, **C**, (the transition state) downhill with a SP of index 2, point **B**, which corresponds to the top of a two-dimensional hill, cf. ref. [21]. Such combination has to be characterized by a VRI (valley-ridge inflection) point [25-37] in between. There are infinitely many gradient lines from point **B** to every neighboring minimum. The detection of the VRI point can be realized by the use of Newton trajectories (NT). The curves bifurcate at VRI points. However, gradient lines do not bifurcate outside stationary points.

It has been shown by Wales [38] and by Quapp [39] that the VRI point is coordinate invariant. (However, it is not invariant on the quantum chemical method to calculate the PES.) If it exists it is on the PES in any coordinate system and characterizes the PES topology. From the saddle point **C** (transition state of index one) on the PES to the tangential direction of the transition vector only one gradient line leaves and this gradient line terminates at the stationary point **B**. This follows from symmetry arguments. Only a bifurcating NT can open the insight into the possibilities of bifurcating reaction pathways which circumvent hilltop **B**. After point **B**, the flow of infinitely many gradient lines goes down to the product minimum. So we have the queer case in that the IRC from the transition state to the product minimum does not consist of only one continuous line but of infinitely many lines.

2. Methods

All calculations to find the stationary points in this paper were performed by standard methods of coupled cluster CCSD, CCSD(T) methods including all electrons (keyword “full”) and the density functional theory method B3LYP in the triple-split basis set 6-311++G(3df,3pd) using the Gaussian 03 software package [40]. Optimization of molecular geometry in stationary points at all levels of approximation has been performed with the convergence criteria "tight". No counterpoise corrections were made for the basis set superposition error (BSSE) [41-44] in calculations. All results refer to the gas phase. The calculations of NTs were coupled with the GamessUS package [45-47] where the B3LYP/6-311G(df,pd) method is used.

We calculate NTs by an Euler-Branin-step method following along the direction of the vector field $\mathbf{A} \mathbf{g}$ of the so called Branin differential equation [48]

$$d \mathbf{x}/dt = \pm \mathbf{A}(\mathbf{x}) \mathbf{g}(\mathbf{x}),$$

where \mathbf{A} is the adjoint matrix of the Hessian, and \mathbf{g} is the gradient of the surface, and t is a curve length parameter. The iteration of the exact value of the VRI coordinates is done by the two methods described in refs [34]. The methods allow us to exactly get the singular NT which meets the VRI point and branches there.

3. Results and discussion

3.1. Stationary points on the CH_5^- and FCH_4^- PES's

The performed quantum chemical calculations show that the PESs of the CH_5^- and FCH_4^- $\text{S}_{\text{N}}2$ reactions (1) have stationary points in the region of the structures **1-9**. The geometric characteristics of these structures are shown in **Figs. 1** and **2**. Total and relative values of the energy, as well as of the values of the zero point energy in the harmonic approximation (ZPE) for the structures of **1-9** and isolated molecules of methane, fluorometane, hydride and fluoride anions are given in Table 1. Structures corresponding to the radicals or results of a system decay are not considered. According to the calculations, the structure of **1**, **5** and **9** corresponds to the minimums ($\lambda=0$), the **2**, **4**, **6** and **8** are saddle points of index one ($\lambda=1$), and the structures **3** and **7** correspond to the top of the "two-dimensional hill" ($\lambda=2$), thus they are saddle points of index two.

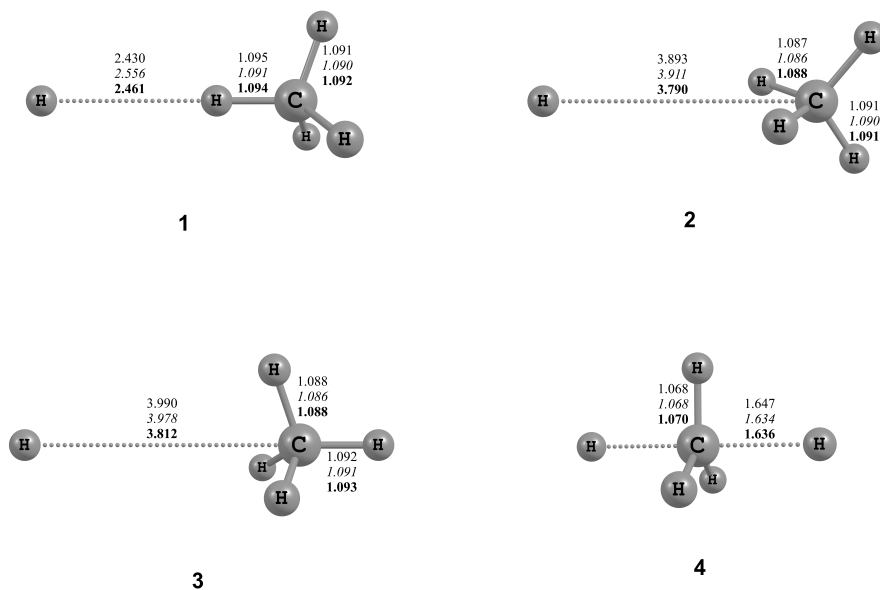


Fig.1. Geometrical parameters for structures **1-4** are predicted by B3LYP/6-311++G(3df,3pd) (plain), CCSD(full)/6-311++G(3df,3pd) (italic) and CCSDT(full)/6-311++G(3df,3pd) (bold) methods. Bond lengths are given in Å.

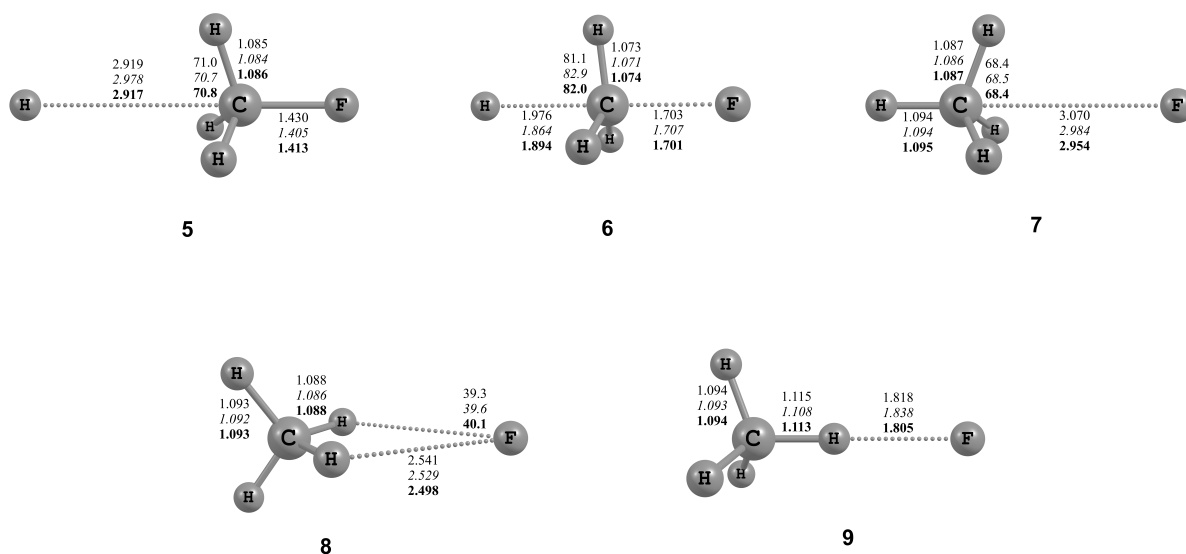


Fig.2. Geometrical parameters for structures **5-9** are predicted by B3LYP/6-311++G(3df,3pd) (plain), CCSD(full)/6-311++G(3df,3pd) (italic) and CCSDT(full)/6-311++G(3df,3pd) (bold) methods. Bond lengths and valence angles are given in Å and degrees respectively.

Table 1. Data* obtained by B3LYP/6-311++G(3df,3pd), CCSD(full)/6-311++G(3df,3pd) and CCSDT(full)/6-311++G(3df,3pd) calculations for structures **1-9**.

STRUCTURE	METHOD	λ	E_{tot}	ΔE	E_{ZPE}	ΔE_{ZPE}	ω_1
1 , C_{3v}	B3LYP	0	-41,0756823	0	0.045400	0	193
	CCSD	0	-40,9822130	0	0.045792	0	163
	CCSD(T)	0	-40,9893578	0	0.045523	0	172
2 , C_{2v}	B3LYP	1	-41,0736309	1.29	0.044791	0.91	i160
	CCSD	1	-40,9806340	0.99	0.045231	0.64	i144
	CCSD(T)	1	-40,9875779	1.12	0.044918	0.74	i154
3 , C_{3v}	B3LYP	2	-41,0732035	1.56	0.044604	1.06	i96
	CCSD	2	-40,9802485	1.23	0.045032	0.76	i95
	CCSD(T)	2	-40,9871359	1.39	0.044750	0.91	i104
4 , D_{3h}	B3LYP	1	-40,9992743	47.95	0.042322	46.02	i1411
	CCSD	1	-40,8951151	54.65	0.042760	52.75	i1650
	CCSD(T)	1	-40,9067059	51.86	0.042220	49.79	i1580

STRUCTURE	METHOD	λ	E_{tot}	ΔE	E_{ZPE}	ΔE_{ZPE}	ω_1
5 , C_{3v}	B3LYP	0	-140.3483166	56.59	0.039893	53.41	146
	CCSD	0	-140.1301027	54.63	0.040737	51.54	137
	CCSD(T)	0	-140.1451098	55.72	0.040388	52.65	147
6 , C_{3v}	B3LYP	1	-140.3382171	62.93	0.039770	59.67	i708
	CCSD	1	-140.1084782	68.20	0.040845	65.18	i985
	CCSD(T)	1	-140.1277473	66.62	0.040255	63.46	i911
7 , C_{3v}	B3LYP	2	-140.4307105	4.89	0.044378	4.52	i174
	CCSD	2	-140.2101321	4.41	0.044838	3.89	i147
	CCSD(T)	2	-140.2264056	4.71	0.044533	4.24	i152
8 , C_{2v}	B3LYP	1	-140.4323104	3.88	0.044637	3.68	i274
	CCSD	1	-140.2112726	3.70	0.045071	3.32	i258
	CCSD(T)	1	-140.2276283	3.94	0.044739	3.60	i273
9 , C_{3v}	B3LYP	0	-140.4385004	0	0.044968	0	204
	CCSD	0	-140.2171621	0	0.045662	0	196
	CCSD(T)	0	-140.2339068	0	0.045279	0	204

* E_{tot} (in a.u.) - total energies (1a.u.=627.5095 kcal·mol⁻¹); E_{ZPE} (in a.u.) - harmonic zero-point correction; λ - the number of the negative hessian eigenvalues; ω_l or $i\omega_l$ (in cm⁻¹) - the smallest or imaginary harmonic vibration frequency; ΔE (in kcal·mol⁻¹) - relative energies (1a.u.=627.5095 kcal·mol⁻¹); ΔE_{ZPE} (in kcal·mol⁻¹) - relative energy including harmonic zero-point correction.

It is important to note that the results obtained by different methods are in mutual agreement with each other and with the data of earlier studies [49,50]. The calculated geometry of methane CH₄ and fluoromethane FCH₃ are also in mutual agreement with MW measurements [51].

3.2. Reaction $CH_4 + H \rightarrow CH_4 + H$

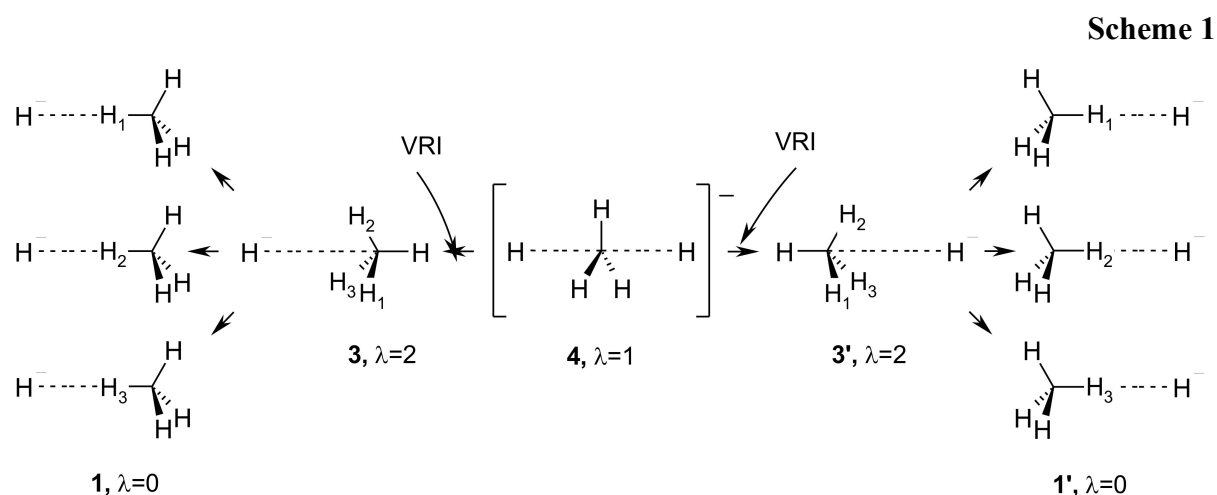
According to calculations, the S_N2 reaction $CH_4 + H \rightarrow CH_4 + H$ begins with the formation of the di-hydrogen bonding complex **1**, having an energy formation ~ 2 kcal·mol⁻¹

(see Table 2). The length H...H bond and the energy formation (see Table 2) in complex **1** is comparable to a similar length and energy in other complexes with H...H bonding [52]. Note that the inclusion of ZPE does not greatly reduce the complex formation energy.

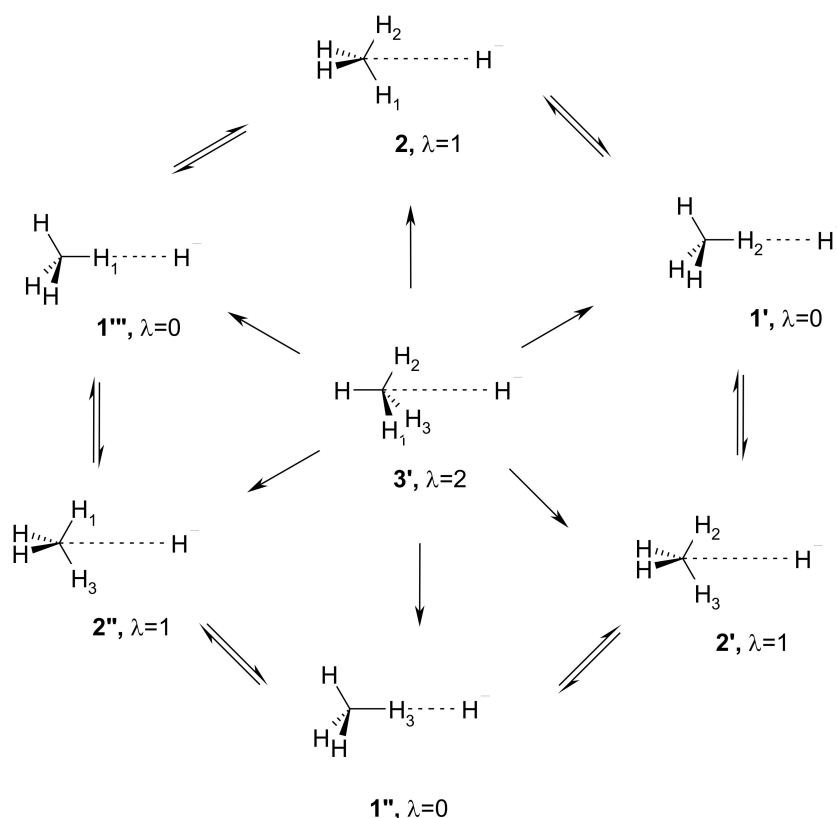
Table 2. The complexes' formation energy* (kcal·mol⁻¹)

Structure	Method	without ZPE	with ZPE
1	B3LYP	2.59	2.06
	CCSD	2.21	1.67
	CCSD(T)	2.56	2.01
5	B3LYP	8.70	8.21
	CCSD	8.41	7.81
	CCSD(T)	8.90	8.30
9	B3LYP	7.79	7.53
	CCSD	7.60	7.14
	CCSD(T)	8.26	7.87

*for **1** – relative to CH₄ + H⁻
 for **5** - relative to FCH₃ + H⁻
 for **9** - relative to CH₄ + F⁻



On the CH₅⁻ PES there are three equivalent minima of **1'**, **1''**, **1'''** with a different orientation of the H...H_{1,2,3}C bonding. These three minima are separated by three transition states **2'**, **2''** and **2'''** corresponding to reactions of reorientation of the hydride ion H⁻ from one HC bond to another (see Scheme 2) with an energy barrier ~ 1 kcal·mol⁻¹ (see Table 1). Note that similar three equivalent (hydrogen-bonding) minima connected by TS were found in [15] however any second order SP was not discovered in the reaction zone.



To follow the gradient reaction path is easy from the saddle point (transition state) **4**. Gradient lines only terminate at stationary points. From the saddle point **4** only one gradient line (steepest descent path) emanates tangentially to the transition vector towards the product (or in the opposite direction towards the reactant), and the gradient line can only terminate, by symmetry reasons, at the neighborhood stationary point **3'** (or in the reverse direction at point **3**), which corresponds to the top of a two-dimensional hill ($\lambda=2$). The C_{3v} point group symmetry for the molecular configuration is preserved along the gradient line down to the next stationary point **3'** (or **3**). An infinite number of gradient lines emanating from point **3'** tangentially to the double degenerate imaginary vector lead to further downhill. All the ways terminate at the three minima **1'**, **1''**, or **1'''**, while only three gradient lines connect the points **3'** of index two with the saddle points **2**, **2'**, or **2''**. **Fig. 3** illustrate this. We calculate the gradient lines for a model analytic function that mirrors the topology of the CH_5^- PES in the region of the reorientation reactions (see Scheme 2).

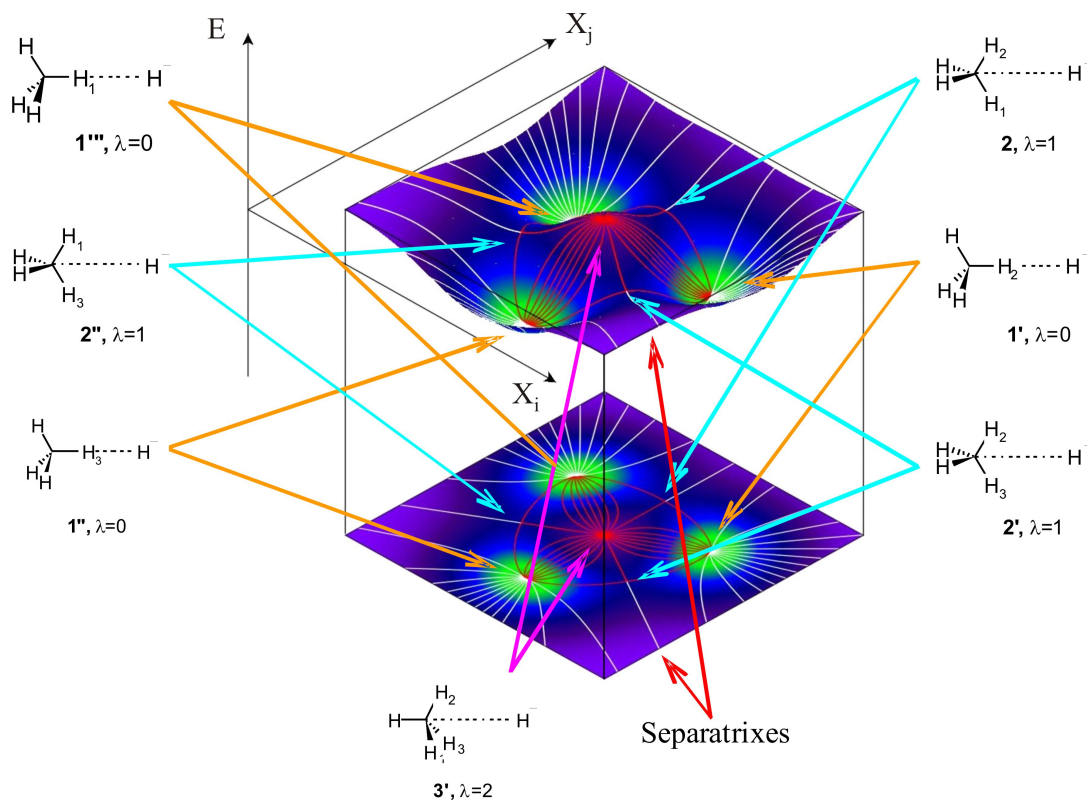


Fig. 3. Surface sections and gradient lines (red or white lines) for a model analytic function which mirrors a two-dimensional part of the CH_5^- PES in the region of the reorientation reactions (see Scheme 2). An infinite number of gradient lines connects point **3'** with each minimum **1'**, **1''**, or **1'''** while only three gradient lines connect **3'** to saddle points in between (transition states) **2**, **2'**, or **2''**. Along these three gradient lines a VRI point does not emerge.

A VRI (valley-ridge inflection) point [25-37] must exist in front of point **3'** (or **3**) on the PES, at which two PES curvatures in the perpendicular direction to the reaction path have to change from a positive to a negative value. At the VRI point the reaction path can trifurcate (or branches) towards the three equivalent minima **1'**, **1''**, or **1'''**. However, the side branches cannot be gradient lines because these lines cannot bifurcate at the slope – it is consistent with the statement of the uniqueness of the IRC-minimum energy path [20]. The gradient path directly connects stationary points, and it cannot branch at the slope of the PES. The bifurcation cannot be described by steepest descent pathways.

3.3. Study of the reaction path bifurcation on the way from **4** to **3**

The bifurcation cannot be described by steepest descent pathways. This is the reason that we change our point of view and use here another kind of curves, the Newton trajectories (NT) [26-29]. A NT is a geometrically defined pathway which may serve as a reaction path.

Geometrically defined means that only properties of the PES are taken into account like in the definition of the SD, however, no dynamical behavior of the molecule is used. Some years ago, the distinguished coordinate along the valley of the minimum was transformed into a new mathematical form [26,27]. The concept is that any preselected gradient direction is fixed

$$\mathbf{g}(\mathbf{x}) / |\mathbf{g}(\mathbf{x})| = \mathbf{r} ,$$

where \mathbf{r} is the unit vector of the search direction, \mathbf{g} is the gradient of the PES, and \mathbf{x} is the current curve point. The search direction may correspond to an assumed start direction of a chemical reaction. For example, it may be the direction between the two minimums of reactant and product. Or it can be the direction along a valley of the minimum, or any other direction. A curve belongs to the search direction \mathbf{r} , if the gradient of the PES always remains parallel to the direction \mathbf{r} at every point along the curve. An infinite number of NTs to different directions crosses the same stationary point but may fill the space between a minimum and an SP. All NTs of the same family concentrate at the same SP. It is simply a consequence of the definition of the NTs: the gradient vector is the zero vector at the stationary points. All search directions can flow into the zero vectors if the gradient disappears. If one imagines the NT to be a curve of the system point driven by a force in a fixed direction, then the NT may indeed fill the gap between the static IRC and dynamical trajectories. However, this is an abstract imagination. A numerical method to get such a curve is the Branin differential equation outlined in the Introduction. Note that a former name of the method was reduced gradient following (RGF) [26,27].

Here, we use the most important property of the NTs: they bifurcate at valley-ridge inflection points of the PES [26-29]. NTs can start like the gradient lines at the SP **4** in the direction of the SP col and can go downhill analogously. The col direction is a stretching of the distance of one outer H atom (the distance CH₆, see structure in **Fig. 4** top right), and the shortening of the distance of the diametric H-atom (the distance CH₂, see structure in **Fig. 4** top right). Along the first steps the curvature of the path is negative. It corresponds with the eigenvalue i1411 in Table 1. Anywhere along the path, this stretching eigenvalue changes into plus values and forms the incoming direction at the structure **3**, an SP of index two. Because the path comes from above, the curvature has to be really positive; this direction works like a normal mode in a minimum. However, the structure **3** is an SP of index two. The two negative eigenvectors now concern the angle and the dihedral of the outer H-atom, H₆. Thus,

before **3**, on the pathway, there must be a change from the positive curvature of these two angle directions into two negative curvatures. NT calculations allow us to exactly detect the region of the PES where the bifurcation takes place. In **Fig. 4** we show a two-dimensional section of the two distances of the outer H atoms, with an inlay for the energy. Two bifurcation points are only depicted by a dot; the two distances themselves do not bifurcate. In contrast, in **Fig. 5**, we show the two-dimensional section of the distance of H₆ and its angle. We found a putative triple point of the path bifurcation. It is not a single bifurcation but a quite complicated net of single ‘normal’ VRI points with bifurcating branches surround it. Often the branches connect the VRIs themselves, others go into the PES mountains, or they are quasi cyclic NTs [53]. The last kind of NTs indicates a flat, but valley without stationary point. At the diverse VRI points either the first eigenvalue, or the second eigenvalue goes individually through zero where the other one stays on a low level. In the region between the VRI points there emerges a larger strip of disappearing numbers of both eigenvalues, thus, the ‘double-zero’ really happens. A deeper discussion of the NT theory for the case should be moved into a next paper.

Altogether, the full region of VRI points contains a transition of the eigenvalues of the outgoing H₆ from positive to negative values, as expected, but the bifurcating branches do not lead into the minimum region of the molecule. This event may emerge at the structure **3** itself building an SP of index two, as well as a bifurcation point. The VRI region is the end of the downhill valley from SP1. However, the valley does not bifurcate there. The bifurcation concerns the uphill ridge from SP2. Its side branches go further uphill as ridges.

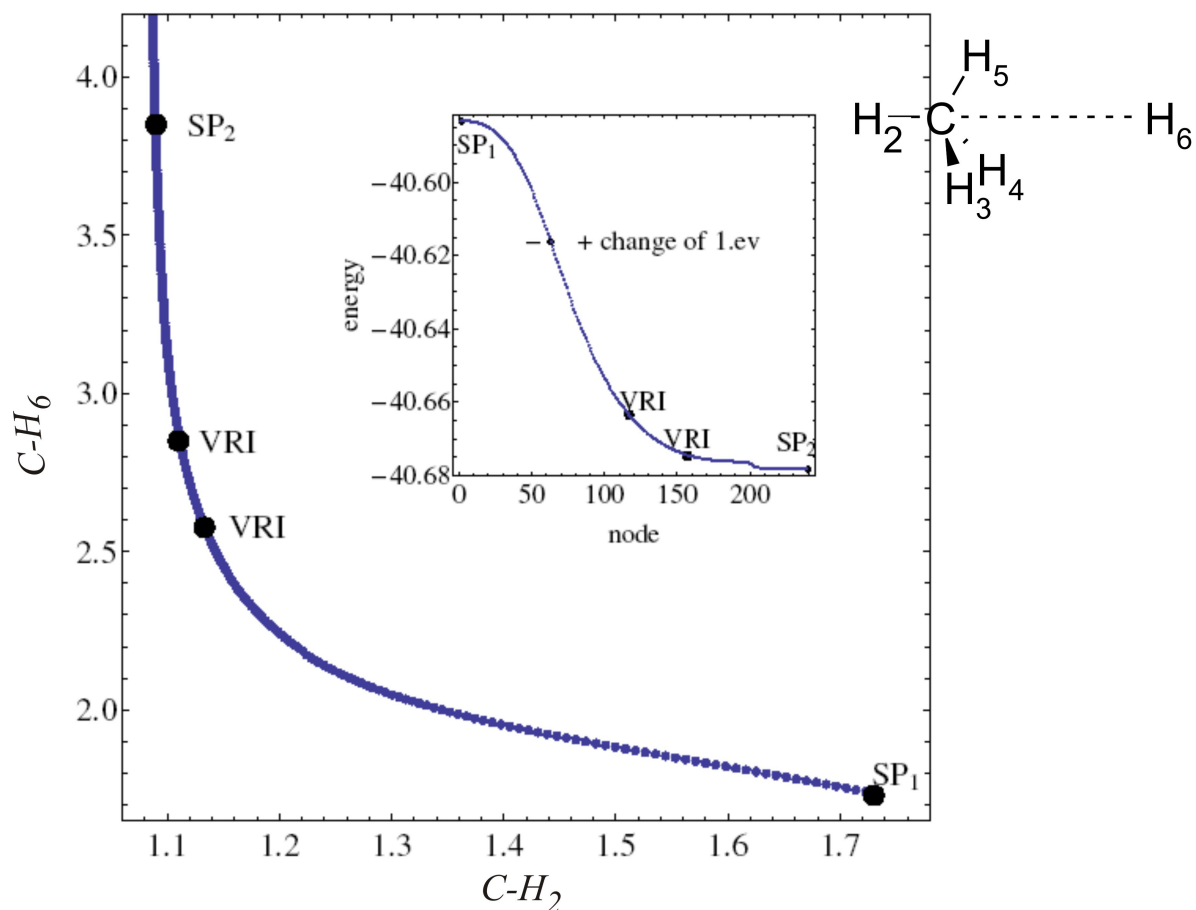


Fig. 4. A singular NT trough the region of the VRI points connecting SP_1 (4) and SP_2 (3) calculated with GamessUS by the B3LYP/6-311G(df,pd) method. Of course, it is only a 2-dimensional projection. The inlay is the energy profile over the NT.

DFT (B3LYP/6-311++G(3df,3pd) calculations of IRC and steepest descent paths also show that VRI point locate in the region of the $C-H_6$ value equal ≈ 2.6 Å. The two projected degenerated negative frequencies of SP_2 (structure 3) in the region $C-H_6 \sim 2.65 - 2.6$ Å along the path are changed from a negative value to a positive one.

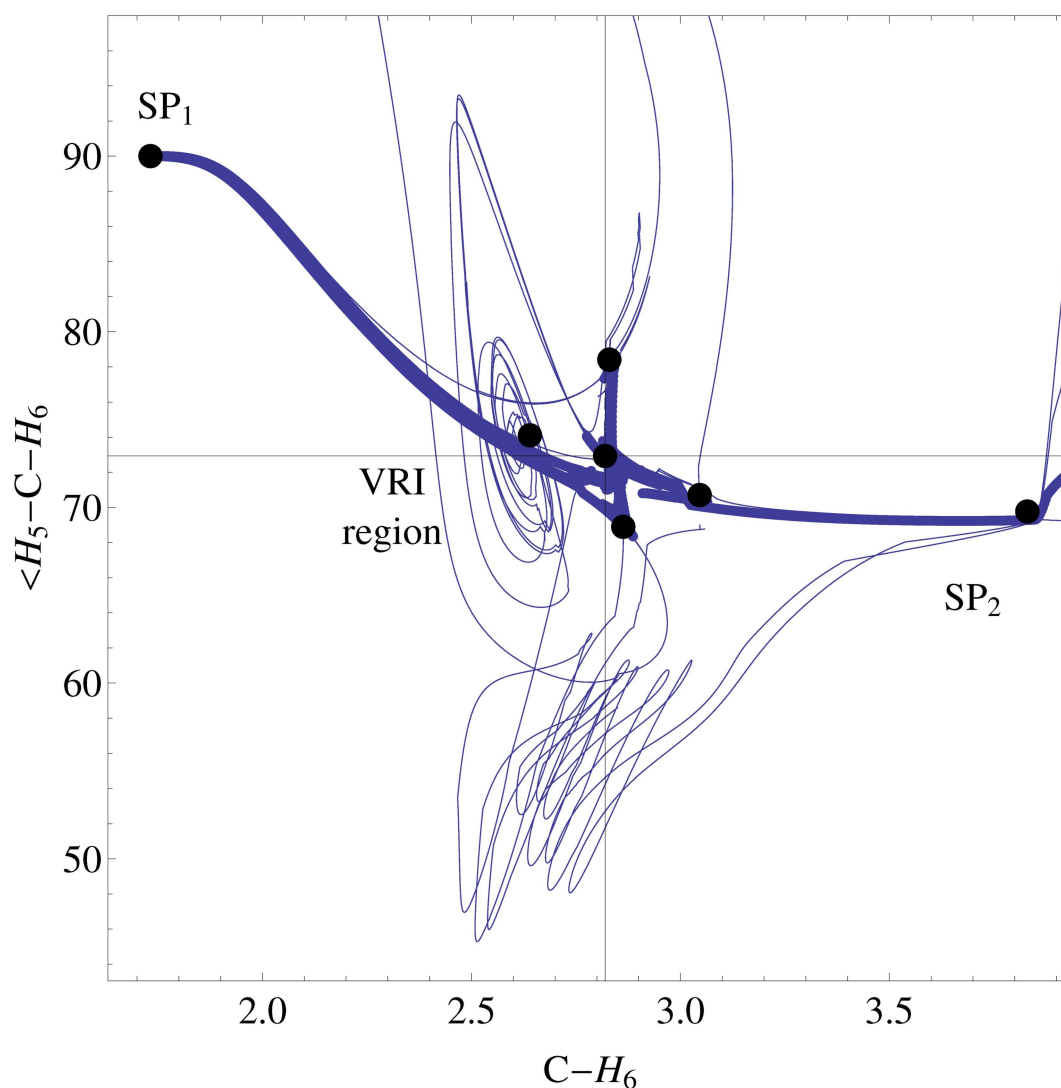


Fig. 5. PES of CH_5^- in the projection into the plane of distance C-H_6 and angle $\text{H}_5\text{-C-H}_6$ (see designation in **Fig.4**). On the pathway from SP_1 to SP_2 emerges a net of VRI points, where the path changes from valley character to a ridge of index two. The SP_1 valley finishes at the first VRI point. There is a singular NT (bold line) through the region which connects the two SPs. Some branches of different bifurcation points are shown by thin lines. They circumvent the region, or escape uphill, or go also downhill, after some cycles, to the SP_2 . NTs can start at SP_2 in every direction.

The two eigenvalues of the angle and dihedral of H_6 are positive before the VRI region, but after the region they both are negative.

3.4. Reaction $H + FCH_3 \rightarrow CH_4 + F^-$

The reaction $H + FCH_3 \rightarrow CH_4 + F^-$ begins with the formation of the complex **5**, stabilized by a hypervalent $H \cdots CF$ interaction [54,55], the energy formation ($\sim 8 \text{ kcal}\cdot\text{mol}^{-1}$) of which is much greater than this in **1** (see Table 2). The distance $H \cdots CF$ is shorter than sum of the van der Waals radii of carbon and hydrogen atoms (3.05 \AA) [56]. Accounting ZPE almost has no effect on the formation of the energy of the complexes. After that the reaction path passes through a transition state **6** of the C_{3v} symmetry, from which analogously, as in the previous case, the gradient reaction path enters a two-dimensional hill top **7**. Before point **7** on the PES as well as in the previous case, there has to be the VRI point. In **Fig. 6** the energy profile is presented (left side picture) along the steepest descent path from the point corresponding to structure **6** (transition state structure) to point **7** (structure corresponding to the top of the two dimensional hill). Along this entire path the C_{3v} symmetry of the structure is conserved. The topological structure of the PES is changed from positive curvature (upper left paraboloid) along two orthogonal directions to the reaction path, to zero curvature (blue plane) at the VRI point, and to negative curvatures after the VRI point (below left inverted paraboloid) till point **7**.

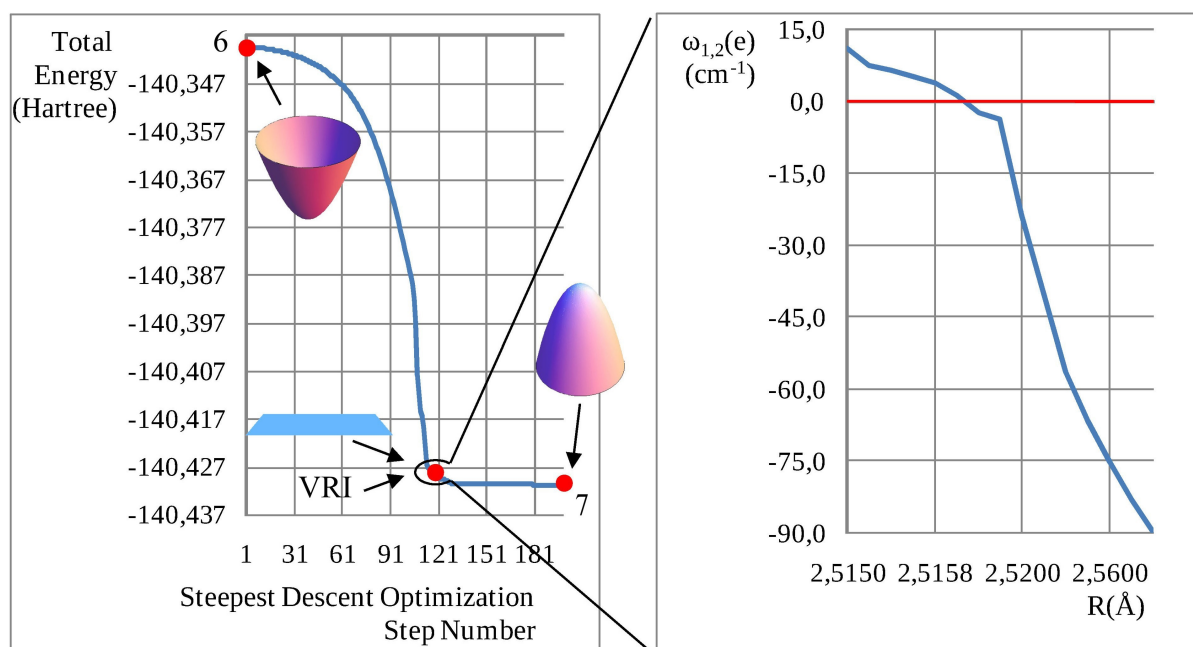
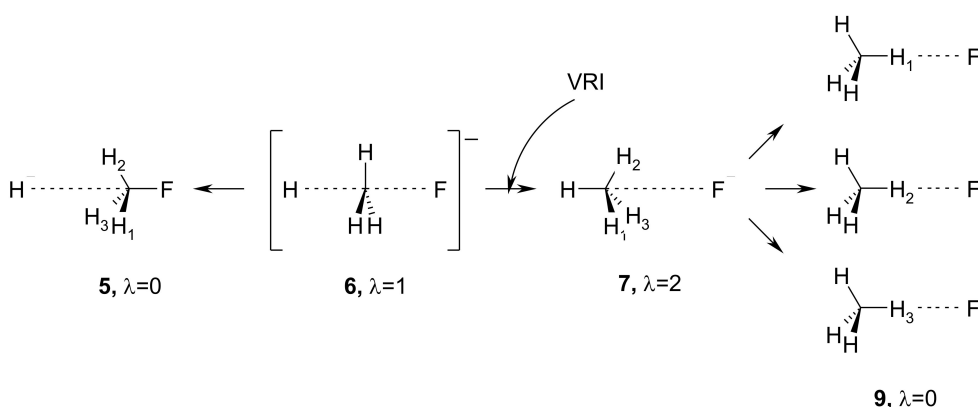


Fig. 6. Calculated by B3LYP/6-311++G(3df,3pd) method energy profile (left side picture) along the steepest descent path from structure **6** (transition state structure) to the point **7** (structure corresponding to the top of the two dimensional hill). In the right side picture is shown the behavior of the two projected double degenerated harmonic frequencies along the steepest descent path in the region of the VRI point. R is the $C \cdots F$ distance. The upper left red

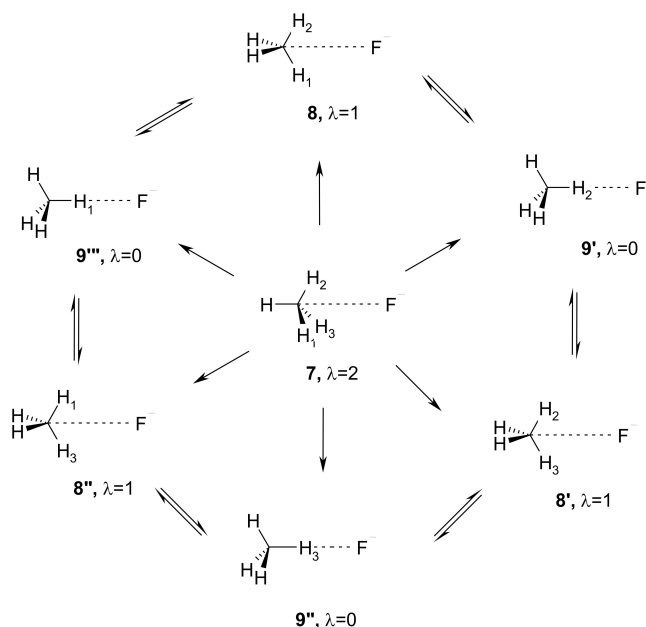
point designates the area near point **6** where the hypersurface has the paraboloid form with positive curvature along two orthogonal directions to the reaction path. At the VRI point this paraboloid convert to a plane and after the VRI point the plane transforms into an inverted paraboloid with two negative curvatures. The right side of **Fig. 6** shows the behavior of the two projected doubly degenerated harmonic frequencies being orthogonal to the reaction path. The displacement goes along the steepest descent path in the small region around the VRI point where the frequencies change their value from positive to negative.

Scheme 3



From the top of a two-dimensional hill **7**, as well as in the previous case, the flow of gradient lines goes down to the product minima **9'**, **9''** and **9'''** (see Scheme 3).

Scheme 4



Out of this stream only three gradient lines, which are the separatrix on the PES, are crossing saddle points (transition states) **8**, **8'** and **8''**(see Scheme 4).

Such an unusual topology of the PES is obtained for the first time and leads to the three following conclusions.

First, there is no limitation of the distribution of stationary points of various types on the PES along the reaction path. An early similar limitation is considered to be the Morse relations [57]. However, the Morse relations only can be applied to the distribution of non-degenerate stationary points in a limited region of the PES of full $3N-6$ dimensions. Thus, the necessity to remove from a consideration all degenerate stationary points and poles out of a consideration makes the application of the Morse relations non-effective for practical use.

Second, it is impossible to introduce strong rules which conserve symmetry elements (symmetry point group) conserving from one minimum (reagent) via the transition state structure to another minimum (product). The usual symmetry conservation rules are based on the presumption that the reaction path which connects two minima (reagent and product) via an SP (transition state structure) is the single continuous smooth minimum energy reaction path (line) which not passes through other stationary points. Indeed in this case, according to Pearson's theorem [58], the symmetry elements are conserved along the reaction path; they contain symmetry elements of both reagent and product. Otherwise, the symmetry point group which is conserved along the reaction path is a subgroup of the symmetry point groups of a reagent, transition state structure and product. However, another stationary point with $\lambda > 1$ appears here, where the reaction path changes its direction on the steepest descent path from the highest transition state.

Third, in the general case there does not exist an unique smooth line depicting the reaction path and connecting the reagent minimum via transition state (or states) with the product minimum and conforms to symmetry conservation rules and the microscopic irreversibility principles.

4. Conclusions

Minimum energy reaction paths (IRC) for the S_N2 nucleophile substitution reactions $CH_4 + H^- \rightarrow CH_4 + H^-$ and $CH_4 + F^- \rightarrow CH_3F + H^-$ triplicate at a lower TS of index two. In between there is a region with many VRI points. After the SP of index two three equivalent families of lines emerge which enter three equivalent minima. Because, the gradient reaction path from a second index saddle point is not one single line, it is a full family of curves, an infinite flow of gradient lines emanating at the three equivalent product minima.

Acknowledgement

This work was supported by the Russian Foundation for Basic Research (grant № 13–03–00203).

References

- [1] S.S.Shaik, H.B.Schlegel, S.Wolfe, Theoretical aspects of physical organic chemistry: the S_N2 mechanism, Wiley, New York, 1992.
- [2] D.K.Bohme, L.B.Young, *J. Am. Chem. Soc.* 92 (1970) 7354.
- [3] D.K.Bohme, G. L.Mackay, J. D. Payzant, *J. Am. Chem. Soc.* 96 (1974) 4027.
- [4] W.Olmsted, J.Brauman, *J. Am. Chem. Soc.* 99 (1977) 4219.
- [5] C.D.Ritchie, G.A.Chappell, *J. Am. Chem. Soc.* 92 (1970) 1819.
- [6] R.A. Rossi, A.B.Pierini, A.B.Penenory, *Chem. Rev.* 103 (2003) 71.
- [7] S.Parthiban, G.Oliveria, J.M.L.Martin, *J. Phys. Chem.* 105 (2001) 895.
- [8] C. Leforestier, *J. Chem. Phys.* 68 (1978) 4406.
- [9] J.Gonzales, W.Allen, H.F.Schaefer, *J. Phys. Chem. A* 109 (2005) 10613.
- [10] P.K.Chattaraj, D.R.Roy, *J. Phys. Chem. A* 110 (2006) 11401.
- [11] P.Manikandan, J.Zhang, W.L.Hase, *J. Phys. Chem. A* 116 (2012) 3061.
- [12] J.Zhang, U.Lourderaj, S.V.Addepalli, W.A. de Jong, W.L.Hase, *J. Phys. Chem. A* 113 (2009) 1976.
- [13] L.Joubert, M.Pavone, V.Barone, C. Adamo, *J. Chem. Theory Comput.* 2 (2006) 1220.
- [14] D.Chakraborty, C.Cardenas, E.Echegaray, A.Toro-Labbe, P.W.Ayers, *Chem. Phys. Lett.* 539 (2012) 168.
- [15] J.Zhang, W.L. Hase, *J. Phys. Chem. A.* 114 (2010) 9635.
- [16] A.Guevara-Garcia, E.Echegaray, A.Toro-Labbe, S.Jenkins, S.A.Kirk, P.W.Ayers, *J. Chem. Phys.* 134 (2011) 234106.
- [17] L.Sun, K.Song, W.L.Hase, *Science* 296 (2002) 875 and references therein.
- [18] S.Giri, E.Echegaray, P.W.Ayers, A.S. Nuñez, F.Lund, A.Toro-Labbe, *J. Phys. Chem. A* 116 (2012) 10015.
- [19] R.M.Minyaev, *Int. J. Quant. Chem.* 4 (1994) 105.
- [20] K.Fukui, *Acc. Chem. Res.* 14 (1981) 363.
- [21] D.Heidrich, W.Quapp, *Theoret. Chim. Act.* 70 (1986) 89.
- [22] R.M.Minyaev, D.J.Wales, *Chem. Phys. Lett.* 218 (1994) 413.
- [23] R.M.Minyaev, D.J.Wales, T.R. Walsh, *J. Phys. Chem. A* 101 (1997) 1384.
- [24] R.M. Minyaev, *Russian Chem. Rev.* 63 (1994) 939.
- [25] R.M. Minyaev, I.V. Getmanskii, W.Quapp, *Russ. J. Phys. Chem.* 78 (2004) 1494.
- [26] W.Quapp, M.Hirsch, D.Heidrich *Theor. Chem. Acc.* 100 (1998) 285.
- [27] M.Hirsch, W.Quapp, D.Heidrich, *Phys. Chem. Chem. Phys.* 1(1999)5291.
- [28] W.Quapp, *J. Theor. Comput. Chem.* 2 (2003) 385.
- [29] W.Quapp, *J. Molec. Struct.* 695-696 (2004) 95.
- [30] W.Quapp, M.Hirsch, D.Heidrich, *Theor. Chem. Acc.* 112 (2004) 40.
- [31] W.Quapp, J.M.Bofill, J. Aguilar-Mogas, *Theor. Chem.Acc.* 129 (2011) 803.
- [32] W.Quapp, J.M.Bofill, *J. Math. Chem.* 50 (2012) 2061.
- [33] J.M.Bofill, W.Quapp, *J. Math. Chem.* 51 (2013) 1099.
- [34] W.Quapp, B.Schmidt, *Theoret. Chem. Acc.* 128 (2011) 47.
- [35] J.M.Bofill, W.Quapp, M.Caballero, *J. Chem. Theory Comput.* 8 (2012) 927.
- [36] B.Schmidt, W.Quapp, *Theoret. Chem. Acc.* 132 (2013) 1305.
- [37] D.H.Ess, S.E.Wheeler, R.G.Iafe, L.Xu, N.Selebi-Olcum, K.N.Houk, *Angew. Chem. Int. Ed.* 47 (2008) 7592.
- [38] D.J.Wales, *J.Chem.Phys.* 113 (2000) 3926.

- [39] W.Quapp, *J. Chem. Phys.* 114 (2001) 609.
- [40] Gaussian 03, Revision E.01, M.J.Frisch, G.W.Trucks, H.B.Schlegel, G.E.Scuseria, M.A.Robb, J.R.Cheeseman, J.A.Montgomery, Jr.,T.Vreven, K.N.Kudin, J.C.Burant, J.M.Millam, S.S.Iyengar, J.Tomasi, V.Barone, B.Mennucci, M.Cossi, G.Scalmani, N.Regga, G.A.Petersson, H.Nakatsuji, M.Hada, M.Ehara, K.Toyota, R.Fukuda, J.Hasegawa, M.Ishida, T.Nakajima, Y.Honda, O.Kitao, H.Nakai, M.Klene, X.Li, J.E.Knox, H.P.Hratchian, J.B.Cross, V.Bakken, C.Adamo, J.Jaramillo, R.Gomperts, R.E.Stratmann, O.Yazyev, A.J.Austin, R.Cammi, C.Pomelli, J.W.Ochterski, P.Y.Ayala, K.Morokuma, G.A.Voth, P.Salvador, J.J.Dannenberg, V.G.Zakrzewski, S.Dapprich, A.D.Daniels, M.C.Strain, O.Farkas, D.K.Malick, A.D.Rabuck, K.Raghavachari, J.B.Foresman, J.V.Ortiz, Q.Cui, A.G.Baboul, S.Clifford, J.Cioslowski, B.B.Stefanov, G.Liu, A.Liashenko, P.Piskorz, I.Komaromi, R.L.Martin, D.J.Fox, T.Keith, M.A.Al-Laham, C.Y.Peng, A.Nanayakkara, M.Challacombe, P.M.W.Gill, B.Johnson, W.Chen, M.W.Wong, C.Gonzalez, J.A.Pople, Gaussian, Inc., Wallingford CT, 2004.
- [41] R.Cammi, R.Bonaccorsi, J.Tomasi, *Theor. Chim. Acta.* 68 (1985) 271.
- [42] F.B.v.Duijnevelt, R. van de Duijneveld, J.H.v. Lenthe, *Chem. Rev.* 94 (1994) 1873.
- [43] G.Lendvay, I.Maer, *Chem. Phys. Lett.* 297 (1998) 365.
- [44] S.Simon, M.Duran, J.J.Dannenberg, *J. Chem. Phys.* 105 (1997) 11024 and references cited therein.
- [45] M.V.Schmidt, K.K.Baldrige, J.A.Boatz, S.T.Elbert, M.S.Gordon, J.H.Jensen, S.Koseki, N.Matsunaga, K.A.Nguyen, S.Su, T.L.Windus, M.Dupuis, Jr.J.A. Montgomery, *J. Comput. Chem.* 14 (1993) 1347.
- [46] M.S.Gordon, M.W.Schmidt, in: C.E.Dykstra, G.Frenking, K.S.Kim, G.E.Scuseria (Eds.), *Theory and Applications of Computational Chemistry, the First Forty Years*, Elsevier, Amsterdam, 2005, p. 1167.
- [47] <http://www.msg.chem.iastate.edu/GAMESS/GAMESS.html>
- [48] F.H. Branin, *IBM J. Res. Develop.* 16 (1972) 504.
- [49] S.Simon, C.A.H.Pierrefixe, M.Bickelhaupt, *Struct. Chem.* 18 (2007) 813.
- [50] P.Maitre, F.Volatron, P.C.Hiberty, S.S.Shaik, *Inorg. Chem.* 29 (1990) 3047.
- [51] J.L.Duncan, *J. Mol. Spectrosc.* 60 (1976) 225.
- [52] V.I.Bakmutov, *Dihydrogen Bonds: Principles, Experiments, and Applications*, John Wiley & Sons, Inc., Hoboken, New Jersey, 2008.
- [53] W.Quapp, J.M.Bofill, M.Caballero, *Chem. Phys. Lett.* 541 (2012) 122.
- [54] V.I.Minkin, R.M.Minyaev, *Chem. Rev.* 101 (2001) 1247.
- [55] R.M.Minyaev, T.N.Gribanova, V.I.Minkin, in: J.Reedijk, K.Poeppelemeier (Eds.), *Comprehensive Inorganic Chemistry II*, Elsevier, 2013, vol. 9, chap. 4.
- [56] J.Emsley, *The Elements*, Clarendon Press, Oxford, 1991.
- [57] J.W.Milnor, M.Spivak, R.Wells, *Morse Theory*, *Ann. Math. Studies* 51, Princeton U. Press, 1963.
- [58] R.G.Pearson, *Theor. Chim. Acta*, 16 (1970) 107.